Characterisation and morphology of biodegradable chitosan / synthetic polymer blends

Maria Mucha*, Joanna Piekielna, Anna Wieczorek

Technical University of Łódź, Faculty of Process and Environmental Engineering, Wólczańska 215, 90-924 Łódź, Poland

SUMMARY: Chitosan has been used to form miscible, biodegradable blends with hydrophilic synthetic polymers as PVA and PEO. Characterisation of the blends by DSC, IR and microscopy analysis was made giving much attention to possible interactions of molecular polar group in the polymer chains. PVA/chitosan are found to be amorphous in the whole range of composition having one glass transition temperature. Molecular interactions in the pair of polymers are connected with amide group of chitosan and hydroxyl groups of PVA. PEO/chitosan blends stay amorphous up to 0.2 weight fraction of PEO. For a higher amount of PEO that polymer crystallises forming a spherulite crystalline structure. We correlate the overall kinetics of crystallisation and melting behaviour of solid, semicrystalline blends PEO/chitosan in the form of thin films for a set of PEO species of different blend composition with a morphological structure of the blends. Negative values of the Flory-Huggins interaction parameter due to specific interactions by hydrogen bonding through ether group of PEO and hydroxyl group of chitosan were evaluated. Amide groups do not participate in the molecular interaction between PEO and chitosan molecules. Avrami equation was applied to describe kinetics of crystallisation of pure PEO and PEO/chitosan blends of various compositions.

Introduction

Chitosan derived from chitin is an important aminopolysaccharide in view of the utilisation of natural polymer resources. Recently, chitosan and its derivatives have attracted much attention, because they have been found to provide a new class of functional polymeric materials as, e. g., selectively permeable membranes [1-2] and biomedical uses [3].

Polymer blends containing biodegradable components have attracted much attention especially in relation to the application in disposable packages industry or medicine. Hydrophilicity of the most non-degradable synthetic polymers has limited miscibility

 CCC 1022-1360/99/$ 17.50+.50/0

with hydrophilic biopolymers and thus it has great influence on the blend preparation and properties. When the non-biodegradable polymer is hydrophilic and water soluble such as poly(ethylene oxide) (PEO) or poly(vinyl alcohol) (PVA) good compatibility with biopolymers can be expected. Some blends of this type such as poly(ethylene oxide) with polylactid acid, poly(D-3 hydroxybutyrate) [3-6] or chitosan [7-9), 28-30] and poly(vinyl alcohol) with chitosan [31-32] have been described.

In this paper IR studies and thermal behaviour of PEO and PVA solid blends with chitosan as a biodegradable component are presented. The present studies are continuation of recent works [9,10]. Here attention will be focused on IR studies and thermal effects observed for the PEO blends with a very low concentration of chitosan, turning to their possible new applications.

When chitosan is dissolved in the acetic solution the following equilibrium takes place:

$$\text{Chit.} - NH_2 + HX \rightarrow \text{chit.-}NH_3^+, X^-$$

Chitosan in the acetic condition is a polyelectrolyte [11] whose charge density depends on pH and degree of deacetylation. The degree of protonation close to 1 is found when pH is lower than 4.5.

In the presented studies 1% acidic chitosan solution with pH lower than 4 was used for the blend preparation by casting method. Obviously, blending the chitosan acetic solution with PEO or PVA aqueous solution makes some pH increase.

PEO and PVA form complexes by strong ionic interactions between polar ether groups (PEO) or hydroxyl groups (PVA) and amino or hydroxyl groups existing in chitosan acetic salt. Our previous results [8] on the rheological behaviour of chitosan/PEO or PVA blend solutions confirmed good compatibility of the blends in the solution with a simultaneous increase of the apparent activation energy for viscous flow with rising concentration of PEO or PVA which reached a maximum value for 0.6 weight fraction of the polymers. A possible explanation for that behaviour was a formation of complex spatial structure due to the molecular ionic interactions and hydrogen bonds. For the amount of PEO or PVA higher than 0.6 decreasing the apparent activation energy for viscous flow was observed. It was explained by possible precipitation of the chitosan

complexes from solution or by change of the condition for the spatial entanglement formation.

In other words, pH in mixed solution induces the deprotonation of glucosamine residues and changes the rotational freedom of amine groups which become more flexible [12]. This increase in flexibility should facilitate the association of the hydrophobic sequences of chitosan resulting in a phase separation of the polymer or complex polymer from the solution.

The solid chitosan blends with PVA are found to be homogeneously amorphous in the whole range of composition. They are miscible having one glass transition temperature whose value changes with composition [10]. In the case of PEO/chitosan solid blends the driving forces due to PEO crystallisation from the homogeneous one-phase solution of both components lead to heterogeneous phase structure which consists of modified PEO spherulites in mixed amorphous regions.

The interaction between the crystalline phase of PEO and mixed amorphous regions via surface free energy considerations is expected to produce an interesting behaviour in the melting phenomena that influences the crystallisation kinetics of semicrystalline component.

Experimental

PEO with molecular weight of 10^4 was purchased from Polysciences Inc. Chitosan was made of α-chitin from Antarctic Krill's shells. It was produced in the Sea Fishery's Institute (Gdynia, Poland) by thermochemical deacetylation of chitin. The average molecular weight was $M_w=4.5*10^5$, deacetylation degree DD=73.3 %. Polyvinyl alcohol (PVA) was a commercial product.

The blends in solution were obtained by mixing the appropriate amounts of both polymer solutions: PEO and PVA aqueous solution of 4 % concentration by weight and chitosan acetic acid (1 %) solution of 1 % concentration by weight. Films ~ 30 μm thick were produced by casting techniques and dried at room temperature for 72 hours and

then under vacuum at 40°C for 6 hours. The PEO/chitosan and PVA/chitosan blends were obtained in the range of composition from 0.01 to 0.9 of chitosan weight fraction.

Thermal analysis was carried out on a Mettler FP 85 differential scanning calorimeter at heating rates equal 10°/min. and various thermal histories. The DSC measurements of PEO blends were done according to the following heating and cooling regimes. The original sample (obtained from solutions by the casting method) was heated at heating rate equal 10°/min. from room temperature T_1 to overheating temperature T_2=90°C. Melting temperature T_{m1} (first run) for PEO crystal formed from solution was recorded. Then the sample was kept for 3 min. at 90°C to remove all residual PEO nuclei. After that a fast cooling to an appropriate crystallisation temperature was applied. The crystallisation occurs for the time needed for the completion of the process at chosen temperature. Then the sample was heated at heating rate 10°/min. from T_C to T_2=90°C. In that way, melting temperature T_{m2} (second run) for PEO crystals formed from the melt was recorded. During the last cooling at cooling rate 10°/min. crystallisation heat and temperature were recorded. The heats of exothermic crystallisation processes (at constant T_C) were drawn and then integrated at various crystallisation times.

Morphological structure was examined using a polarising optical microscope with crossed polarises, video camera and computer MultiScan analysis system. Infrared (IR) measurements were done using Spectrometer I Specord M89 (Zeiss Jena).

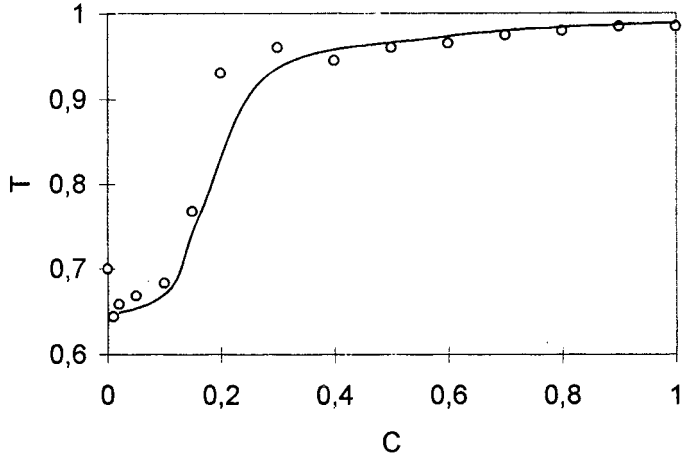

Fig. 1: Laser light relative transmittance T through blends with PEO versus weight fraction of chitosan $T=I/I_0$.

Morphology

PVA/chitosan blends were amorphous and transparent in the whole range of composition. In the case of semicrystalline blends of PEO/chitosan light transmittance (He-Ne laser) drawn versus blends composition shows in Figure 1 good transparency of the blend film for 0.2-1.0 weight fraction of chitosan.

PEO crystallises from the solution in spherulitic structure. Optical microphotographs (analysed by computer) presented in Figure 2 show modification of the spherulite morphology of PEO with an increasing amount of chitosan in the blends. The spherulite structure of PEO was clearly formed in the blends containing from 0.1 to 0.6 weight fraction of chitosan. For higher concentration of chitosan some ordered crystalline regions of PEO are still present. Above value of 0,9 weight fraction of chitosan the blend stays amorphous. The increasing presence of chitosan in the blend causes a limitation of nucleation process of PEO; thus the number of PEO nuclei decreases, and the size of spherulites increases.

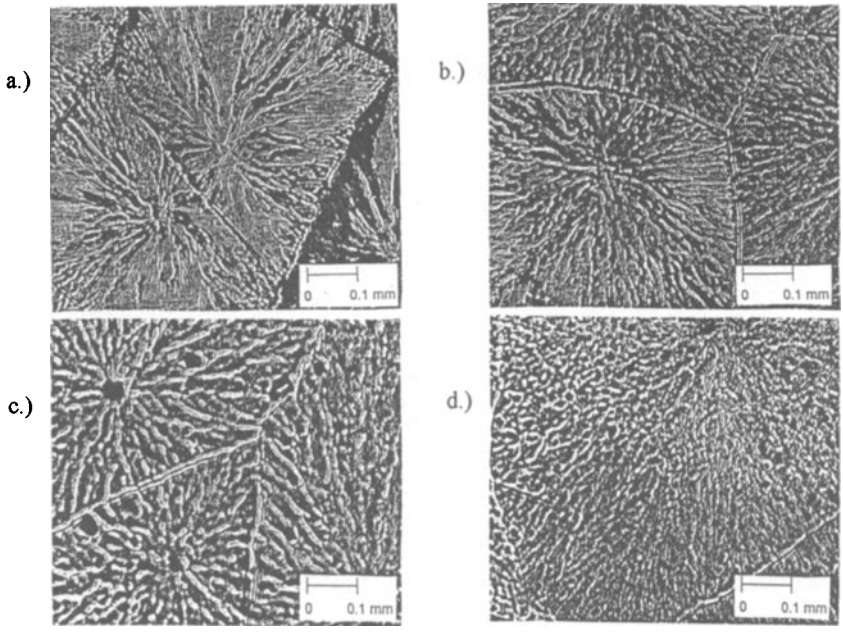

Fig. 2: Microphotographs of PEO/chitosan blends of various chitosan contents a.) 0.2, b.) 0.4, c.) 0.5, d.) 0.6 taken by polarising microscope, video camera and computer image analyser system.

Figure 3 shows a size distribution curve (number of nuclei versus chitosan concentration) calculated from the number of spherulites found in 8 mm^2 of the film area plotted versus weight fraction of chitosan in the blends. Chitosan molecules well miscible with PEO molecules stay incorporated in the interlamellar regions of PEO spherulites. There is no evidence that chitosan forms separated domains in the intra- or interspherulitic areas.

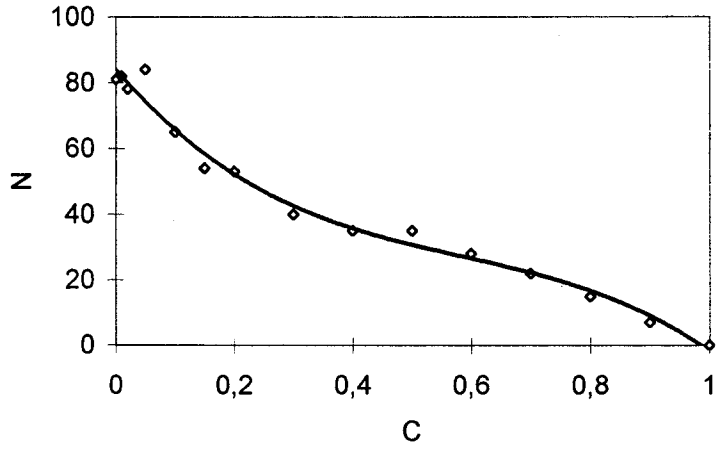

Fig. 3: Number of PEO spherulites in 8 mm^2 of the film area (-size distribution) drawn versus weight fraction of chitosan

IR results

The purpose of our IR studies was to provide direct information on the interaction effects existing in the miscible blends of PEO or PVA with chitosan. IR spectra of all samples in the form of thin films were run on Specord instrument with computer counting of band heights. In the case of PEO/chitosan blends thin films were prepared up to 0.5 weight fraction of PEO. Because of high crystallinity of PEO, the samples with higher PEO content were non-transparent and brittle. Their IR measurements were made using KBr dish. The following characteristic bands were taken into account:

1. For chitosan [14-16]:

the hydroxyl band at 3400 cm^{-1} taken as an internal standard to correct some differences in the film thickness;

the amide I band at 1652 cm^{-1}; the $-NH_3^+$ band at 1568 cm^{-1}; the -CH stretching band at 2880 cm^{-1}

2. For PEO:

the $-CH_2$ scissoring band at 1480 cm^{-1} taken as a standard band

the -C-O-C- stretching band at 1280 cm^{-1} and at 840 cm^{-1}

3. For PVA:

the $-CH_2$ scissoring band at 1480 cm^{-1} taken as a standard band

the -C-O-C- (stretching) band at 1250 cm^{-1} and 820 cm^{-1}.

No shift of the bands was found in the whole range of blend compositions observed elsewhere [30] for amide band. Some of the absorption bands observed in PEO/chitosan blends can be recognised as involved in the intermolecular interactions of the blend components. In the case of poly(ethylene oxide)/chitosan some authors [7] proposed the formation of the intermolecular hydrogen bonds between OH groups in chitosan molecules and ether links in PEO. Similarly, chain connectivity by hydrogen bonds has been proposed by others [17] in the case of PEO/poly(4-vinyl phenol) where ether oxygen competes for phenolic hydroxyl. The strong band at 1564 cm^{-1} (in our case 1568 cm^{-1}) attributed to $NH_3^+OOC^-$ in chitosan, "also exists" in PEO/chitosan and does not participate in the intermolecular bonding between PEO and chitosan [7].

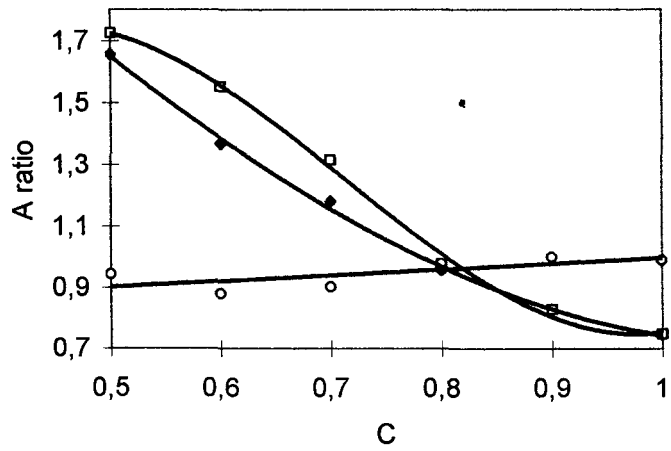

Fig. 4: Absorbance ratio of bands at 1568 to 3400 cm^{-1} characteristic for chitosan molecules (explanations in the text) at ◆ 2880/3400, □ 2880/1568 and ○ 1568/3400 drawn versus weight fraction of chitosan in PEO/chitosan blends

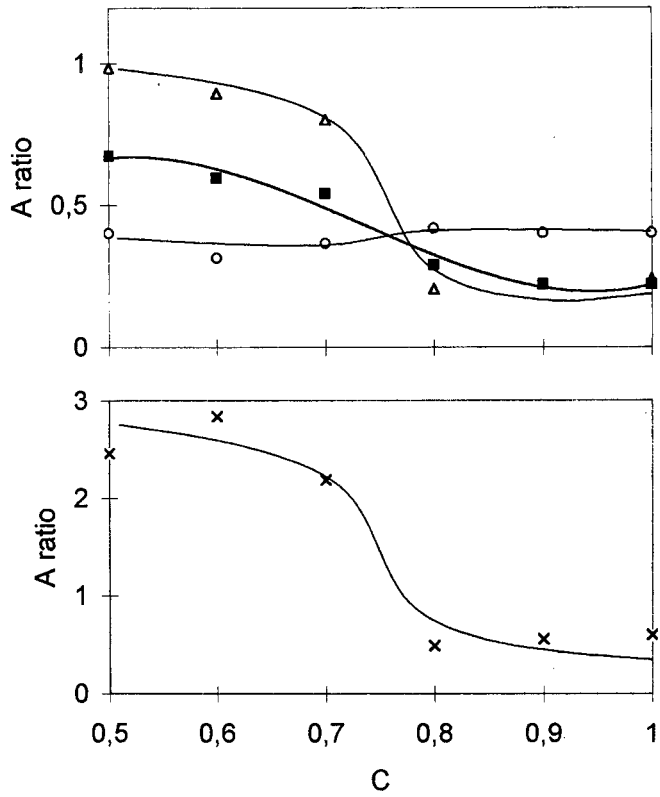

Fig. 5: Absorbance ratio of bands (at ▲1280, ■ 840 and O 1480 cm^{-1}) to band of hydroxyl group (at 3400 cm^{-1}) and × 1280/1480 versus weight fraction of chitosan

In our case for PEO/chitosan blends the absorbance (log 1/T in the band height) of the chosen bands or absorbance ratio is drawn versus weight fraction of chitosan (in the range from 0.5 to 1.0) (Figures 4,5). Because hydroxyl band at 3400 cm^{-1} is characteristic of chitosan molecules the band was taken as an internal standard. (The band at 3499 cm^{-1} is strong and its absorbance increases linearly with rising chitosan content.) The band absorbance ratio 1568/3400 increases linearly with increasing chitosan content in the blend (Figure 4). It can support the other conclusions [7] that - NH_3^+ ions do not participate in the intermolecular interactions in the formation of ionic complexes. In the case of C-O-C groups characteristic of PEO their absorbance or absorbance ratio do not change proportional to the weight fraction of PEO content. The ether groups are obviously involved in intermolecular interactions by possible hydrogen

bonds. Figure 5 shows that for the blends containing up to 0.25 weight fraction of PEO the C-O-C characteristic bands are not distinguished. The PEO molecules are so well dispersed in chitosan matrix (PEO does not crystallise) and their interactions due to hydrogen bonding with chitosan molecules forming matrix are strong enough to form a complex structure. The results have supported our microscopic observations and DSC analysis. It is important to pay attention to the role of water in the complex formation in chitosan itself and in PEO/chitosan blends. On the basis of DSC and dielectric spectroscopy studies of chitosan the authors found that some amount of water associated by chitosan was nonfreezable (no ice peak was observed) and formed water chitosan bonds with hydroxyl bonds of chitosan molecules. The amount of nonfreezable water does not depend on amino content (deacetylation degree). Water molecules can restrict the motion of chitosan molecules and reduce chain flexibility (observed in dielectric measurements). The effect of water on complex formation of PEO with chitosan should be recognised. Our microscopic observations together with DSC studies confirmed the importance of water in the intermolecular connections between PEO and chitosan molecules.

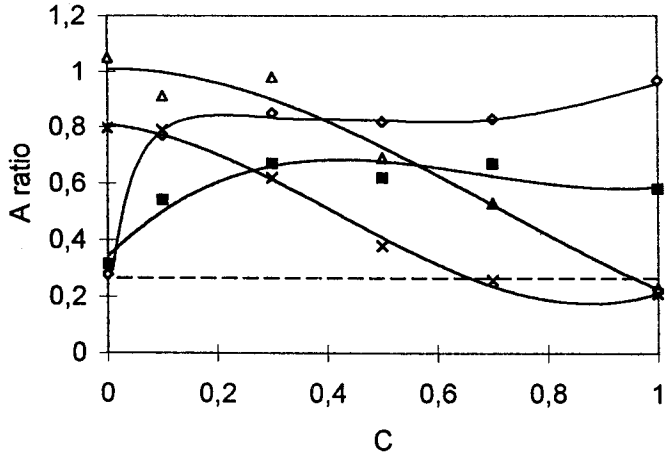

Fig. 6: Absorbance ratio of characteristic chitosan (◇ 1560 and ■ 1652 cm^{-1}) and PVA (Δ 1250 and × 820 cm^{-1}) bands to hydroxyl group band using as a standard band taken at 3400 cm^{-1} versus weight fraction of chitosan for PVA/chitosan blends. A ratio equal 0.3 is a level of background

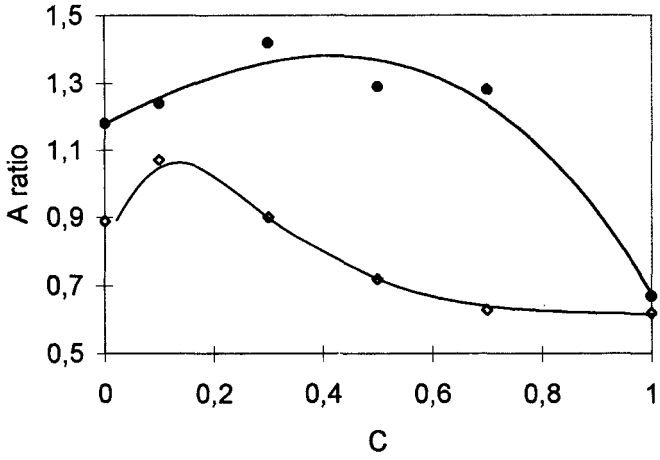

Fig. 7: Absorption ratio of C-O-C (at ◇ 820 and ● 1250 cm^{-1}) bands to CH_2 band (at 1480 cm^{-1}) characteristic of PVA versus weight fraction of chitosan in PVA/chitosan blends

Because in the case of PAV/chitosan blends all film samples for IR studies were of the same thickness we could take the value of height of absorption band for comparison. Figures 6-8 show the absorption and absorption ratio of the characteristic bands for PVA/chitosan blends. Figure 6 shows that the ratio of absorption band at 1560 and 1652 cm^{-1} to hydroxyl band at 3400 cm^{-1} remains constant for weight fraction of chitosan higher than 0.3. Absorption of bands at 1250 and 820 cm^{-1} characteristic of C-O-C groups of PVA decrease with increasing chitosan content. Value of absorption ratio equal 0.3 is a background level. Figure 7 presents clearly the change of absorption band ratio of C-O-C groups at 820 cm^{-1} and 1250 cm^{-1} to 1480 cm^{-1} with chitosan content. The linear character of plot of band absorption at 1480 cm^{-1} with blend composition confirms lack of intermolecular interactions through the band (Figure 8) but non-linear plots of PVA bands 1250 cm^{-1} or at 820 cm^{-1} (Figure 7) and the chitosan bands at 1560 cm^{-1} and at 1652 cm^{-1} result from existing intermolecular interaction through the amino groups of chitosan and hydroxyl group of PVA.

Height of hydroxyl band at 3400 cm^{-1} is almost constant in the whole range of composition due to the presence of OH groups characteristic of both polymers (and possible existence of absorbed nonfreezable water molecules).

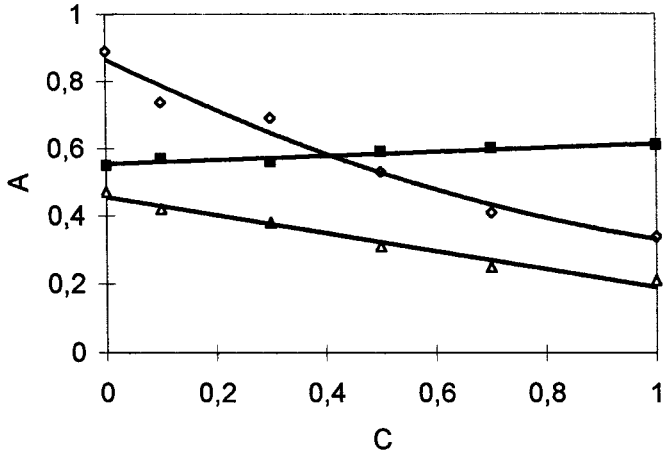

Fig. 8: Linear dependence of absorption bands at ■ 1480 cm^{-1} and Δ 3400 cm^{-1} (hydroxyl band) versus weight fraction of chitosan in PVA/chitosan blends; and their ratio ◇

The IR analysis and problems of intermolecular interactions in chitosan blends with PEO and PVA in the presence of water molecules will be considered in the next paper. That problem remains controversial in the cited literature.

PEO melting temperature and the thermodynamic interaction parameter calculations

DSC thermograms taken in the first run after solution crystallisation of PEO are shown in Figure 9. Some residual amount of water absorbed by chitosan can influence also melting temperature T_m of PEO. Figure 10 presents values of melting temperature, heat and entropy of melting for PEO in the blends found in a first and second DSC runs. The presence of chitosan in the blend perturbs the nucleation and crystallisation processes of PEO both upon evaporation of solvent or upon cooling from the molten state as well as the melting behaviour upon heating. The intermolecular interactions between two polymers alter the surface free energy and perturb the chain folding characteristic of PEO [18,19]. For concentration of chitosan in the blend higher than 0.8, the heat and entropy of melting decreases to zero, the system remains completely amorphous.

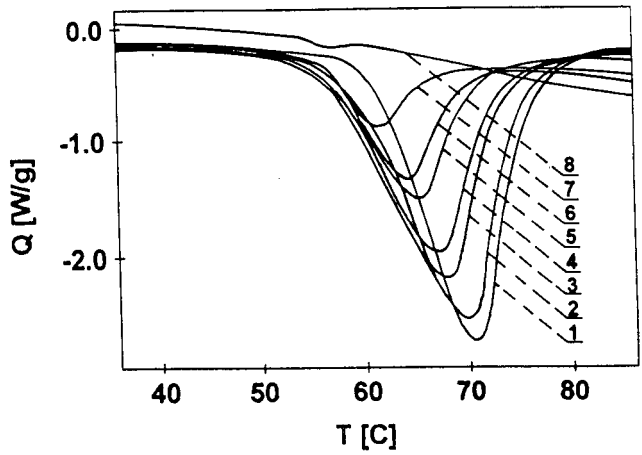

Fig. 9: DSC thermograms taken in the first run for crystallisation of PEO from solution in the region of melting temperature of PEO drawn for various fractions of chitosan (1-0, 2-0.01, 3-0.1, 4-0.2, 5-0.5, 6-0.6, 7-0.8, 8-0.9) (first run). Heating rate equal 10°/min.

It is known that miscibility of polymers in blends is controlled by thermodynamic factors [20]. The Flory-Huggins thermodynamic interaction parameter χ_{12} characterises the interaction in free energy of mixing and is used as a measure of the excess enthalpic and entropic contributions to potentially favourable mixing. The more negative the parameter the stronger the interaction. Several techniques [21] have been used to determine the Flory-Huggins parameter of miscible polymer blends. In this work we used melting point depression to determine χ_{12} from the equilibrium and non-equilibrium melting temperatures of blends. If the conformational entropic contribution to the mixing process is neglected even though the molecular weight of some PEO samples is not very high, the interaction parameter can be determined from widely used Nishi Wang [22], equation 1.

$$1/T_{mb}^{0} - 1/T_{m}^{0} = -\{ R\, V_{2u}/\Delta H_{2u}\, V_{1u} \}\, \chi_{12} V_1^2 \qquad 1$$

Tm^0 - equilibrium melting temperature of pure PEO

T_{mb}^0 - equilibrium melting temperature of PEO in the blends with chitosan

V_1 - volume fraction of chitosan

V_{1u} - repeated unit molar volume of chitosan V_{1u}=132.5 cm^3/mol

V_{2u} - repeated unit molar volume of PEO V_{2u} = 39.3 cm^3/mol

ΔH_{2u} - enthalpy of fusion of completely crystalline PEO ΔH_{2u} = 9782.2 J/mol

R - gas constant R = 8.314 J/mol K

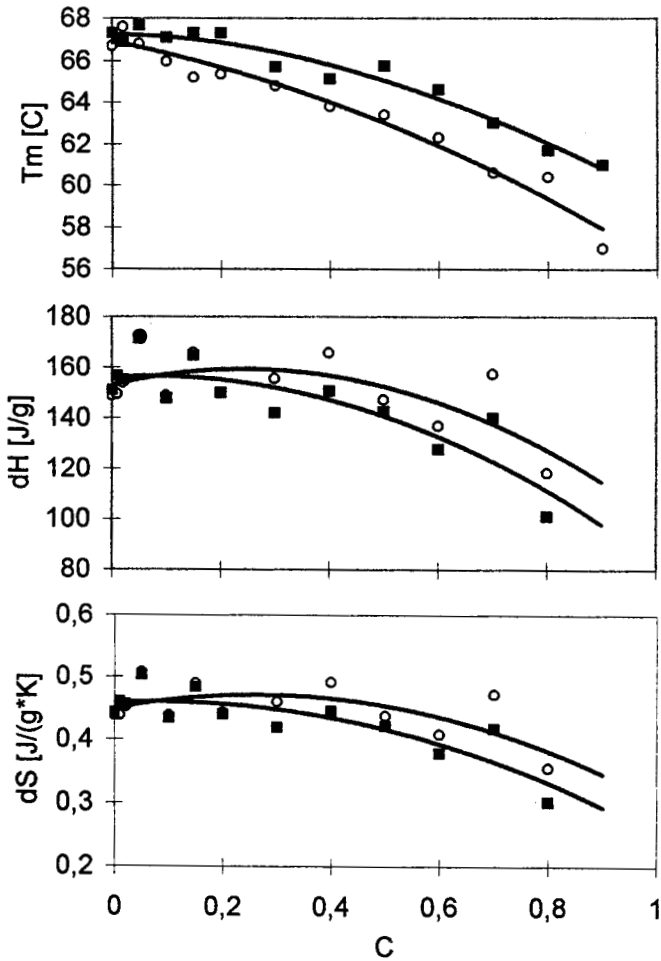

Fig. 10: Temperature (Tm), heat (dH) and entropy (dS) of PEO melting in the blends versus weight fraction of chitosan obtained in O first (melting of virgin samples obtained from solution) and ■ second runs (melting after crystallisation at 48°C)

For calculation of the thermodynamic interaction parameters χ_{12} , T_{mb} and T_m were taken instead of T_{mb}^0 and T_m^0. Average values of χ_{12} are found: 0.37 from the first run

and -0,29 from the second run (-0.56 and –0.25 was found before [9]. These negative values indicate that PEO and chitosan are miscible in the amorphous phase of PEO due to specific interactions between the components. These values are of the same magnitude as those in other miscible systems [23-25].

The original blends obtained by casting from a solution exhibit better miscibility (lower χ_{12}) than the ones obtained from a melt. Separation of chitosan content from interlamellar regions of PEO in the course of annealing process of the blends close to the melting temperature of PEO is observed.

Kinetics of PEO crystallisation, half time of crystallisation, $\sigma\sigma_e$ calculations

Figure 11 presents an example of DSC thermograms of isothermal crystallisation of PEO in the blends with chitosan of various weight fractions of chitosan drawn at T_C=48°C.

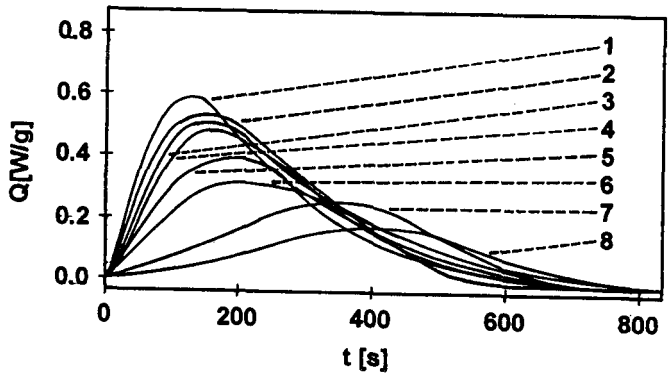

Fig. 11: Isothermal crystallisation curves obtained for pure PEO and its blends with chitosan of various weight fractions c of chitosan (1-0, 2-0.02, 3-0.1, 4-0.15, 5-0.2, 6-0.3, 7-0.4, 8-0.5) at the same crystallisation temperature Tc=48 °C

For all the samples studied the dependence of the crystallisation half-period on supercooling temperature $1/T\Delta T$ ($\Delta T=T_m^0-T_C$) where T_m^0 is the equilibrium temperature of melting PEO (pure and in the blends) and T_C-crystallisation temperature has been obtained. For example in the case of PEO/chitosan in 1:1 ratio the values of $t_{0.5}$ are much higher than for pure PEO at the same supercooling.

Kinetic data has been analysed in terms of the bi-exponential equation 2 for growth rate ν at crystallisation temperature T_c as follows:

$$\nu = \nu_0 \bullet \exp. [- (\Delta G^* + \Delta G_\eta) / k \bullet T_c] \qquad 2$$

where ΔG^* and ΔG_η are the free enthalpy of formation of critical size nucleus and free enthalpy of activation for diffusion of crystalline element across the phase boundary, respectively.

At high temperature ΔG_η is constant. At low temperature ΔG_η rapidly increases as the glass temperature is approached (3).

$$\Delta G_\eta / k \bullet T_c = a + b /(T_c - T_0) \qquad 3$$

where T_0 is the temperature at which no further transport can take place.

Taking the constancy of the $\Delta G_\eta/k \bullet T$ values in the close crystallisation temperatures under study (T_g of PEO equal about -50°C) and setting $\ln \nu = - \ln t_{0.5}$ [27] equation 4 is obtained:

$$\ln t_{0.5} = \text{cons.} + \Delta G^* / k \bullet T_c \qquad 4$$

For secondary or heterogeneous nucleation, ΔG^* is given by equation 5 :

$$\Delta G^* = 4 \bullet \sigma \bullet \sigma_e \bullet b_0 \bullet T_m^0 / \Delta h_f \bullet \xi_c \bullet \Delta T \qquad 5$$

where σ and σ_e - side and end surface free energies respectively, T_m^0 is the equilibrium melting temperature, ΔT - supercooling $= T_m^0 - T_c$.

For PEO and its blends the following values were taken: single layer thickness $b_0=4.65*10^{-10}$ m and $\Delta h_f \bullet \xi_c = \Delta H_f = 2.64*10^5$ kJ/m^3. [26]

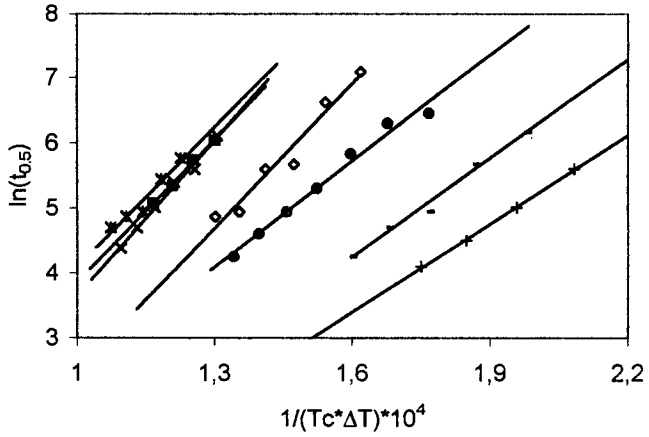

Fig. 12: Temperature dependence of the half-period of crystallisation for various weight fractions of chitosan (◇ 0, ■ 0.1, × 0.3, * 0.4, ● 0.5, + 0.7, - 0.8). $\Delta T=T_m^0-T_c$ - supercooling, T_m^0 – equilibrium melting temperature of PEO in blends, T_c - crystallisation temperature

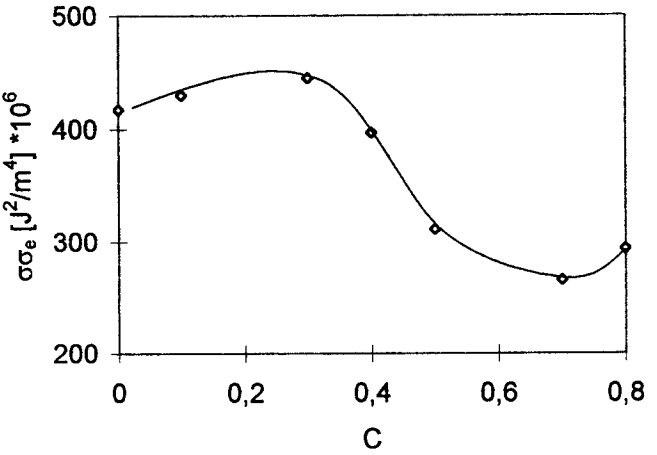

Fig. 13: $\sigma\sigma_e$ plot versus weight fraction of chitosan

From the slopes of kinetic lines (Fig. 12) using equations 4 and 5 $\sigma\bullet\sigma_e$ values were calculated. Figure 13 presents $\sigma\bullet\sigma_e$ plot versus chitosan concentration in PEO/chitosan

blends. A small decrease of the $\sigma \bullet \sigma_e$ value in comparison to pure PEO for low chitosan concentration results from lowering of the energy barrier for nucleation process due to additional orientation effect forced by specific interactions between polar groups of both polymers. For the blend with chitosan content higher than 0.4 the PEO crystalline structure appears poorer. Spherulite structure is modified significantly and disappears completely for c higher than 0.8. It is also reflected in a sharp decrease of T_m and crystallinity degree.

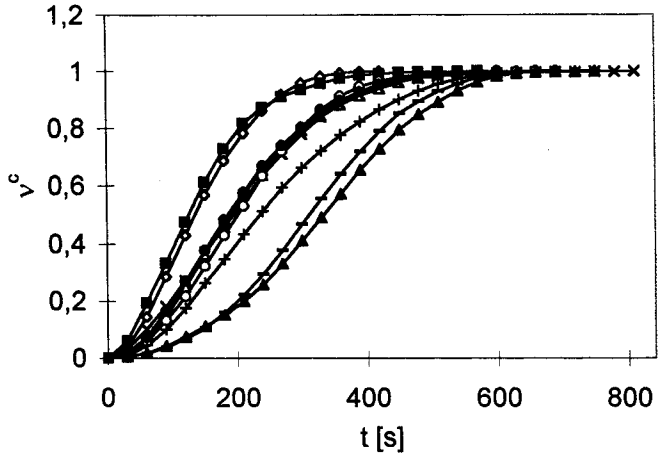

Fig. 14: Kinetic curves drawn for the blends of PEO/chitosan at T_c=48°C, (◇ 0, ■ 0.01, Δ 0.02, × 0.05, o 0.1, ● 0.15, + 0.2, - 0.4, ▲ 0.5), ν_c-conversion degree; $\nu_c = X(t)/X(\infty)$; X(t) and X(∞) crystallinity degree at time t and at the end.

Kinetics of PEO crystallisation, Avrami plots

In general the development of crystallinity ν^c in the phase transformation from melt to crystal can be represented by the Avrami equation 6 :

$$1 - \nu^c(t) = \exp.[-K \bullet t^n] \qquad 6$$

where K and n - Avrami parameters, t - time.

For athermal nucleation and three-dimensional linear crystal growth which is typical for the blends with crystallising component the value of parameter n≅2 in the case of circular lamellar and n=3 for spherical growth is predicted [27].

Calorimetry is easily used to measure crystallinity as a function of time. Assuming a complete crystallisation. The Avrami equation can be written in the form of equation 7:

$$\log \{- \ln [1 - v^c (t)]\} = \log K + n \bullet \log t \qquad 7$$

Figure 14 shows the examples of kinetic curves $v^c=f(t)$ drawn for PEO/chitosan blends of various compositions obtained at T_C=48°C. The linear Avrami plots in the log/log form (data from Figure 14) for various blend compositions are found. The Avrami exponent calculated from the slopes whose average value n=1.9-2.2, appears to be independent of the crystallisation temperature and blend composition studied. The strong decrease of log K (equation 7) (proportional to rate constant of crystallisation) with increase of the crystallisation temperature and weight fraction of chitosan in the blends (Figure 15) are observed.

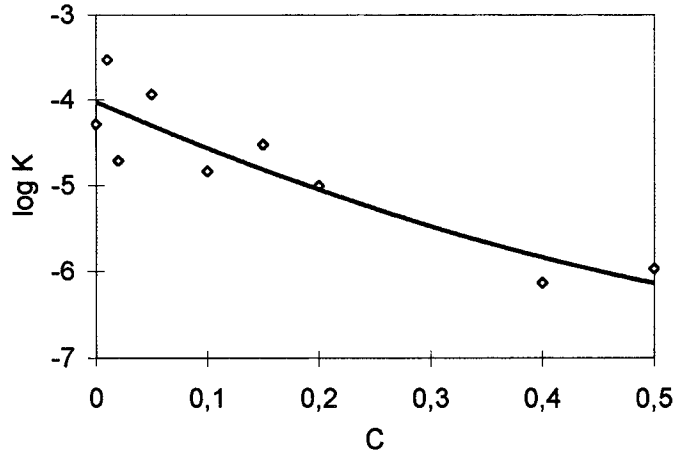

Fig. 15: log K (from Avrami plots) versus weight fraction of chitosan.

Some remarks on the applications of biodegradable chitosan blends

a.) for selective membranes preparation

Chitosan blends in a film form were prepared by blending PEO or PVA aqueous solutions with chitosan acetate solution in an appropriate amount. The blends were obtained in the composition ranging from 0.5 to 0.9 of chitosan weight fraction. Membranes ~ 10 μm thick were produced by casting techniques and initially dried at room temperature for 72 hours. Then PEO or PVA was carefully removed from the films by extraction with ammonia water and rinsed with water, the procedure leads to deactivation of chitosan acetate molecules. It allows to form chitosan films of controllable size of pores to be used as selective membranes. The membranes are keep in wet condition.

The effect of initial PEO or PVA content on permeability of membranes is found. The influence of transmembrane pressure on water permeability for the membranes was measured. The results show a considerable increase of permeate volume for the membranes containing initially PEO or PVA. Thus "structure gaps" intensify fluid flow process in comparison with a pure chitosan membrane.

b.) for paper coating

Our recent studies are concerned with the properties of paper coated with chitosan (solution of various chitosan concentrations 1-3% by weight). The casting technique allowed chitosan to penetrate inside paper, strengthening its structure. Cross-section of the samples, however, shows some part of chitosan remaining on the surface of paper thus creating hermetic film layer. All paper properties like breaking and tearing strength, burst resistance, elongation at break are developed for chitosan-coated paper in comparison to non-coated and commercially PE-coated one.

Mechanical properties of paper enriched with chitosan (10% by weight) by casting wet paper in amount of 10% by weight were much better than those in the paper containing no fillers. PVA/chitosan blends are also used as fillers and coatings for paper. The results of chitosan applications mentioned above will be discussed in separate publications.

Conclusions

Water soluble synthetic polymers PEO and PVA were blended by mixing their solutions with acidic solution of chitosan.

The blends prepared by casting method are found miscible and homogeneous in the whole range of compositions in the case of PVA/chitosan blends (one glass transition temperature is observed) and up to about 0.2 weight fraction of PEO which is a crystallising component of the blend. Miscibility of the blend components are induced by the presence of intermolecular interactions between PEO and chitosan molecules by hydrogen bonding between hydroxyl groups of chitosan and ether oxygen of PEO or PVA and chitosan molecules by hydrogen bonding in which hydroxyl groups of PVA and amide group of chitosan participate (infrared results). In the case of PEO/chitosan blends (DSC results) the evaluation of the negative value of the Flory-Huggins interaction parameter via analysis of the melting point depression shows good compatibility of both components in the amorphous phase. Chitosan molecules rejected in front of growing PEO crystals growth remain incorporated in interlamellar amorphous regions of PEO spherulites (microscopic results). The value of the specific free energy $\sigma \bullet \sigma_e$ of PEO crystals changes with increasing chitosan content. A small initial decrease (c to 0.1) in comparison to pure PEO crystals can be due to lowering of the energy barrier for a nucleation process (by orientational effect) and a faster overall rate of PEO crystallisation. A further small increase of $\sigma \bullet \sigma_e$ to a nearly constant value can be explained by an impeded effect of chitosan molecules leading to the decrease of PEO crystallisation rate. In the case of c values higher than 0.5, the value of $\sigma \bullet \sigma_e$ decreases. The chitosan molecules start to incorporate between crystallites of PEO. PEO crystals appear small and imperfect which is also reflected in decreasing their T_{mb}° and the crystallinity degree values.

Avrami equation can be applied to the description of the crystallisation kinetics of PEO in the PEO/chitosan blends under study. Avrami exponent $n \cong 2.0 \pm 0.2$ was calculated in a broad range of crystallisation time, crystallisation temperature and the blend composition pointing to a heterogeneous (athermal) nucleation mechanism and three-dimensional crystal growth of PEO remaining in the blends.

Film forming biodegradable PVA and PEO/chitosan blends can found interesting applications in selective membrane formation and paper coating.

References

1. T. Seo, H. Ohtake, T. Kanbara, K. Yonetake, T. Iijima, *Makromol. Chem.* **92**, 2447 (1991)
2. T. Seo, H. Ohtake, T. Kanbara, K. Yonetake, T. Iijima, *J. Pol. Sci.* **58**, 633 (1995)
3. P. Calvo, C. Remunan-Lopez, J.L. Vila-Jato, M. J. Alonso, *J. Pol. Sci.* **63**, 125 (1997)
4. H. Younes, D. Cohn, *Eur. Pol. J.* **24**, 765, (1988)
5. H. Avella, E. Martuscelli, *Polymer* **29**, 1731 (1988)
6. A. J. Nijenhuis, E. Colstee, D.W. Grijpma, A.J. Pennings, *Polymer* **26**, 5849 (1996)
7. A. Wrzyszczynski, Qu Xia, L. Szosland, E. Adamczak, L.A. Linden, J.F. Rabek, *Polymer Bulletin* **34**, 493, (1995)
8. M. Mucha, *Macromolecular Chem. Phys.* **198**, 471 (1997)
9. J. Piekielna, M. Mucha, *Inż. Chem. Proc.* **19**, 145 (1998)
10. J. Piekielna, M. Mucha and M. Szwarc; *Advances in Chitin Science vol II 7th ICCC* Ed A. Domard, J. Andre Publ. 539, (1997)
11. J. Desbrieres, M. Milas and M. Rinando *Chitin World*, Proc. of 6th Int. Conf on Chitin and Chitosan, Wirtschaftsverlag NW Verlag für neue Wissenschaft GmbH, 73(1997)
12. K. Katoaka, H. Koyo and T. Tsuruta, *Macromol,* **28,** 3336 (1995)
13. M. Kakizaki, Y. Anada and T Hideshima *Chitin World*, Proc. of 6th Int. Conf on Chitin and Chitosan, Wirtschaftsverlag NW Verlag für neue Wissenschaft GmbH, 183, (1997)
14. J.G.Domszy and G.A.F. Roberts, *Macromol. Chem.*, **186**, 1671 (1985)
15. T. Sannan, K. Kurita, K. Ogura and Y. Ivakura, *Polymer*, **19**, 458, (1978)
16. M.C. Ferreira, M.R. Marvao, M.L. Duarte and T. Nunes *Chitin World*, Proc. of 6th Int. Conf.on Chitin and Chitosan, Wirtschaftsverlag NW Verlag für neue Wissenschaft GmbH, **480**, (1997)
17. P.C. Painter, B. Veytsman, S. Kumar, S. Shenoy, J.F. Graf, Y. Xu and M.M. Coleman, *Macromol.*, **30**, 932, (1997)
18. Qin Chuan, A.T.N. Pires, L.A. Belfiore, *Polymer Communications* **31**, 177 (1990)
19. C.P Buchley, A.J. Kovacs, *Colloid Poymer Sci.* **46**, 254 (1976)
20. O. Olabasi, L.M. Robeson, M. Shaw, *Polymer - Polymer Miscibility*, New York, Academic Press (1979)
21. B. Riedl, R.E. Prud'homme, *Polymer Eng. Sci.*, **24**, 1291 (1984)
22. T. Nishi, T.T. Wang, *Macromolecules,* **21**, 3038 (1988)
23. E. Martuscelli, M. Pracella, W.P. Yue, *Polymer,* **25**, 1097 (1984)
24. P. Pendrosa, J.A. Pomposo, E. Calahorra, M. Cortazar, *Polymer*, **36**, 3889 (1995)
25. J.J. Sotele., V. Soldi, A.T.N. Pires, *Polymer,* **38**, 1179 (1997)
26. K.D. Petrenko, V.P. Privalko, Yu.S. Lipatov, *Polymer,* **31**, 1283 (1990)
27. B. Wunderlich, *Macromolecular Physics,* **2**, Crystal nucleation, Growth, Annealing, New York, Academic Press (1976)
28. W. Zhao YuL, X.Zhong, Y. Zhang, J.Sun; *J. Macromol. Sci,* Phys., **334,** 231 (1995)
29. N. Augelowa, N.Monolova, T. Zlateva, I. Rashkov, V. Maximova, S. Bogadnova, *Chitin World*, Proc. of 6th Int. Conf on Chitin and Chitosan, Wirtschaftsverlag NW Verlag für neue Wissenschaft GmbH, 537, (1997)
30. W Wang, G. Roberts, *Advances in Chitin Science,* **2** ,561 (1997)

31. H.S. Blair, J. Guthrie, T. Law, P. Turkington, *J. Appl. Pol. Sci.*, **33,** 641, (1987)
32. Y. Kuranchi, T. Yanai, K. Ohga, *Chem. Lett.*, 1411, (1991)